ELSEVIER

Biophysical Chemistry 59 (1996) 341–349

Biophysical Chemistry

Complexes of myosin subfragment-1 with adenosine diphosphate and phosphate analogs: probes of active site and protein conformation

Brigitte C. Phan [a,b], Pearl Cheung [a,b], Walter F. Stafford [c,d], Emil Reisler [a,b,*]

[a] *Department of Chemistry and Biochemistry, University of California, Los Angeles, CA 90095, USA*
[b] *Molecular Biology Institute, University of California, Los Angeles, CA 90095, USA*
[c] *Boston Biomedical Research Institute, 20 Staniford Street, Boston, MA 02114, USA*
[d] *Department of Neurology, Harvard Medical School, Boston, MA 02115, USA*

Received 25 April 1995; revised 17 July 1995; accepted 25 July 1995

Abstract

Previous work has revealed phosphate-dependent differences in the complexes formed from myosin subfragment-1 with adenosine diphosphate (S1 · ADP) and aluminum fluoride (AlF_4^-) or beryllium fluoride (BeF_x) [Phan and Reisler, Biophys. J., 66 (1994) A78], with the former resembling more the S1** · ADP · P_i state while the latter resembles more the S1 · ATP state. In this work, the conformations of the S1 · εADP · AlF_4^- and S1 · εADP · BeF_x complexes were examined by nucleotide chase and collisional quenching experiments. εADP release from S1 · εADP · AlF_4^- was slower than that from S1 · εADP · BeF_x. However, acrylamide titrations of S1 · εADP · AlF_4^- and S1 · εADP · BeF_x showed little difference in nucleotide protection from quenching between the two complexes. This contrasts with the earlier observation on phosphate analog-dependent changes in the reactivity of the SH_1 group on S1. To confirm phosphate-related perturbation of the SH_1–SH_2 sequence, emission spectra of fluorescein (IAF)-labeled SH_1 and IANBD-labeled SH_2 were recorded for S1 complexes with nucleotides and phosphate analogs. Considerable differences were found between the BeF_x and AlF_4^- complexes with S1 · MgADP for both SH_1- and SH_2-labeled proteins. These results are consistent with a recent crystallographic study of S1 complexes with ADP and phosphate analogs [Fisher et al., Biophys. J., 68 (1995) 19S] and the idea that the opening of the nucleotide cleft on S1 does not change much during ATP hydrolysis [Franks–Skiba et al., Biochemistry, 33 (1994) 12720], while significant changes in the SH_1–SH_2 region accompany phosphate cleavage.

Keywords: Myosin subfragment-1; Active site; Chelating ion; Proteins; Protein conformation

1. Introduction

It is a privilege to contribute to this special issue of Biophysical Chemistry, dedicated to the memory

* Corresponding author.

SSDI 0301-4622(95)00127-1

of Bill Harrington and honoring him as a scientist, educator, mentor, and a friend. Twenty years ago Bill Harrington's group proposed the first model linking the function of myosin to an interplay between the reactive SH_1 and SH_2 cysteines (cysteine 707 and 697 of rabbit skeletal myosin, respectively) and the nucleotide and actin binding sites on myosin [1]. Today, as much as then, it appears that the clarification of the dynamic connection between these sites is crucial to the understanding of the myosin motor.

A recent molecular model for muscle contraction by Rayment and Holden [2], based on the crystallographic structure of S1 (myosin subfragment-1), has attributed the driving force of muscle contraction to the cyclical opening and closing of the nucleotide pocket. According to this model, a major shape change in the nucleotide pocket occurs during adenosine triphosphate (ATP) hydrolysis, when the active site closes around the base of the nucleotide to produce a conformationally bent myosin head [2]. This hypothesis was supported by recent observations that the ATP binding pocket is closed and/or tightened during ATP hydrolysis [3]. However, in another study which probed the conformation of the active site of S1 by using fluorescence quenching methods, no significant changes were detected in the solvent accessibility of fluorescent nucleotide analogs bound to the active site during the ATPase cycle [4]. Subsequent crystallographic studies on the structures of the truncated Dictyostelium S1 (S1dC) complexed with the phosphate analogs beryllium fluoride (BeF_x) and aluminum fluoride (AlF_4^-) have detected structural differences between the S1dC · MgADP · BeF_x and S1dC · MgADP · AlF_4^- complexes [5], suggesting that significant changes, including the bending of S1, may occur due to phosphate cleavage. Consistent with the crystallographic observations, an independent study of chemical reactivities of SH_1 and SH_2 thiols (Cys-697 and Cys-707 on S1) has suggested conformational differences between the S1 · MgADP · BeF_x and S1 · MgADP · AlF_4^- complexes, with the former resembling the prehydrolyzed state S1 · MgATP and the latter the $S1^{**}$ · MgADP · P_i state [6].

The objective of the present study was to explore the environment of the nucleotide moiety of the S1 · ADP · BeF_x and S1 · ADP · AlF_4^- complexes in solution. Our results show that while changes at the phosphate site induce significant conformational changes in the SH_1–SH_2 sequence, they do not perturb much the adenine moiety of the nucleotide site.

2. Materials and methods

2.1. Reagents

ADP, dithiothreitol (DTT), $BeCl_2$, aluminum chloride, and NaF were purchased from Sigma (St. Louis, MO). 1-N^6-ethenoadenosine diphosphate (εADP), iodoacetamido fluorescein (IAF), and 4-*N*-(iodoacetoxy)ethyl-*N*-methylamino-7-nitrobenz-2-oxa-1,3-diazole ester (IANBD) were purchased from Molecular Probes (Junction City, OR). Crystalline acrylamide was obtained from BioRad (Richmond, CA). Millipore-filtered distilled water and analytical-grade reagents were used in all experiments.

2.2. Proteins

Myosin from rabbit psoas muscle was prepared according to Godfrey and Harrington [7]. Subfragment-1 (S1) was prepared by chymotryptic digestion of myosin as described by Weeds and Pope [8] and was used as a mixture of S1(A1) and S1(A2). Rabbit skeletal muscle actin was prepared in G-actin buffer (0.5 mM β-mercaptoethanol, 0.2 mM ATP, 0.2 mM $CaCl_2$ and 5 mM Tris, pH 7.6) by the procedure of Spudich and Watt [9]. G-actin was polymerized by the addition of 2 mM $MgCl_2$. Protein concentrations were determined spectrophotometrically by using the following extinction coefficients at 280 nm: S-1, $\varepsilon^{1\%} = 7.5\ cm^{-1}$; actin, $\varepsilon^{1\%} = 11.5\ cm^{-1}$.

2.3. ATPase activities

Ca^{2+}- and K^+(EDTA)-activated ATPase activities of S1 were determined according to Kielley and Bradley [10].

2.4. Chase experiments

The stability of the modified S1 · εADP · analog complexes was examined by monitoring the dissocia-

tion of the fluorescent nucleotide analog εADP from S1. Briefly, exhaustively dialyzed S1 (25 μM for the Ca complexes and 5 μM for the Mg complexes) was incubated for 30 min at 25°C with $MgCl_2$ (2 mM) or $CaCl_2$ (2 mM), εADP (20 μM) and either $AlCl_3$ (500 μM) and NaF (10 mM) or $BeCl_2$ (200 μM) and NaF (5 mM). The standard solvent contained 40 mM KCl, 25 mM 1,4-piperazinediethanesulfonic acid (PIPES), pH 7.0. The fluorescence of εADP was measured in the presence of acrylamide (100 mM) which preferentially quenches free εADP [11]. The chase of εADP bound to S1 was carried out with ADP (2.0 mM) or actin (30 μM).

2.5. Acrylamide titrations

The accessibility of εADP to collisional quenchers was examined by titrating εADP with acrylamide. The S1 · εADP · analog complexes in the presence of either Mg^{2+} or Ca^{2+} were allowed to form at room temperature as described for the chase experiments. S1 and εADP concentrations were 15 and 10 μM for the Mg and 25 and 10 μM for the Ca complexes, respectively. The fluorescence intensities of εADP in various complexes were measured as a function of increasing acrylamide concentrations.

All fluorescence measurements of εADP were conducted at 25°C in a Spex Fluorolog Spectrophotometer (Spex Industries, Edison, NJ) at excitation and emission wavelengths of 315 nm and 415 nm, respectively.

2.6. Data analysis

The titration data were corrected for dilution effects and displayed as Stern–Volmer plots in which the initial fluorescence divided by the observed fluorescence was plotted as a function of acrylamide concentration [12]. The Stern–Volmer constants of the free and bound εADP were determined by fitting the data to Eq. 1 [13]:

$$F_o/F = 1/\left[\left(F_f/(1+K_f)[Q]\right) + \left(F_b/(1+K_{SV})[Q]\right)\right] \quad (1)$$

where F_f, F_b represent the fluorescence intensities of the free and bound nucleotide in the absence of quencher Q and K_f and K_{SV} represent their respective quenching constants.

The concentration of free nucleotides was measured following sedimentation of a portion of the sample through a semipermeable membrane with a molecular cutoff of 10–30 kDa that allowed passage of the free nucleotide but not that of the protein and bound nucleotide. The fluorescence of the solution that had passed through the membrane was then measured and the concentration of the free nucleotides was determined from appropriate calibration plots.

2.7. SH_1 modification by IAF

S1 was labeled with IAF as described by Reisler [14]. Briefly, S1 (27.5 μM) was reacted with IAF (500 μM) in 30 mM KCl, 25 mM Tris · HCl, pH 8.0 for 1 h at 0°C. The reaction was stopped by the addition of DTT (2 mM) and the extent of SH_1 labeling was checked by measurements of the K^+(EDTA)– and Ca^{2+}–ATPase activities. In all preparations, after 1 h of modification, at least 95% of SH_1 were modified. Excess reagent was removed by overnight dialysis at 4°C. The IAF-S1 was then incubated with various nucleotides (2 mM MgADP, 3 mM MgATP) and analogs (2 mM MgATPγS). The beryllium fluoride and aluminum fluoride complexes were formed by 30-min incubation of IAF-S1 with $MgCl_2$ (2 mM), ADP (1 mM), and $AlCl_3$ (500 μM) and NaF (10 mM) or $BeCl_2$ (200 μM) and NaF (5 mM). The emission spectra of IAF-labeled S1 · nucleotide complexes were recorded at excitation wavelength of 365 nm.

2.8. SH_2 modification by IANBD

S1 was labeled with IANBD as described by Root and Reisler [15]. This reagent is specific for the SH_2 group in the presence of actin and MgADP. Briefly, S1 (15 μM) in 30 mM KCl, 25 mM Tris · HCl, pH 8.0 was reacted with IANBD (60 μM) overnight at 4°C in the presence of actin (60 μM), $MgCl_2$ (5 mM) and ADP (2 mM). The specificity of labeling was checked by measurements of the K^+(EDTA)– and Ca^{2+}–ATPase activities of S1 at 37°C . After the reaction was stopped by DTT (2 mM); KCl (0.3 M), $NaPP_i$ (2 mM) and ATP (3 mM) were added to dissociate S1 from actin. The two proteins were then separated by centrifugation. The supernatant, which

contained S1, was dialyzed overnight versus 30 mM KCl, 25 mM Tris · HCl, pH 8.0. The IANBD-modified S1 was then incubated with various nucleotides and analogs (as described for IAF modification of S1) and the emission spectra of the labeled S1 · nucleotide complexes were recorded at an excitation wavelength of 472 nm.

3. Results

3.1. Stability of the S1 · εADP · BeF_x and S1 · εADP · AlF_4^- complexes: ADP chase experiments

The overall rate of the Mg–ATPase reaction is determined by the breakdown of the key intermediate S1** · ADP · P_i [16]. The S1** · ADP · P_i state is presumably also formed during the Ca^{2+}–ATPase reaction of myosin. However, the Ca^{2+}-liganded intermediate is less stable and breaks down at a much higher rate (20–50 times more rapidly) than Mg^{2+}–S1** · ADP · P_i [17,18]. Therefore, in principle, the chelating cation should be useful in linking the phosphate analogs with specific states of the myosin ATPase. To this end, the stability of S1 · ADP · BeF_x and S1 · ADP · AlF_4^- complexed with Mg^{2+} and Ca^{2+} was determined by ADP chase. The rationale for these experiments relied on the preferential quenching of free etheno ADP (εADP), a fluorescent ADP analog, by acrylamide [11]. The release of εADP from the nucleotide pocket in the presence of BeF_x and AlF_4^- was monitored by chasing the bound εADP with ADP and monitoring the resulting time-dependent fluorescence changes. The rate of εADP release reflects the dissociation of the phosphate analog, which is the rate-limiting step on the nucleotide dissociation pathway [19].

Fig. 1 shows the release of εADP from the S1 · εADP · BeF_x and S1 · εADP · AlF_4^- complexes in the presence of either Mg^{2+} or Ca^{2+}. The S1 · Mg εADP · AlF_4^- complex is much more stable than S1 · Mg εADP · BeF_x (Fig. 1a). The dissociation rates of BeF_x and AlF_4^-, obtained by fitting the fluorescence decrease to a single exponential expression, were $1.94 (\pm 0.01) \times 10^{-4}$ s^{-1} and $1.14 (\pm 0.01) \times 10^{-5}$ s^{-1}, respectively. As shown in Fig. 1b, the S1 · Ca εADP · BeF_x complex dissociated at a much faster rate than S1 · Ca εADP · AlF_4^-, their k_{off} values were $2.11 (\pm 0.03) \times 10^{-2}$ s^{-1} and $1.15 (\pm 0.01) \times 10^{-5}$ s^{-1}, respectively.

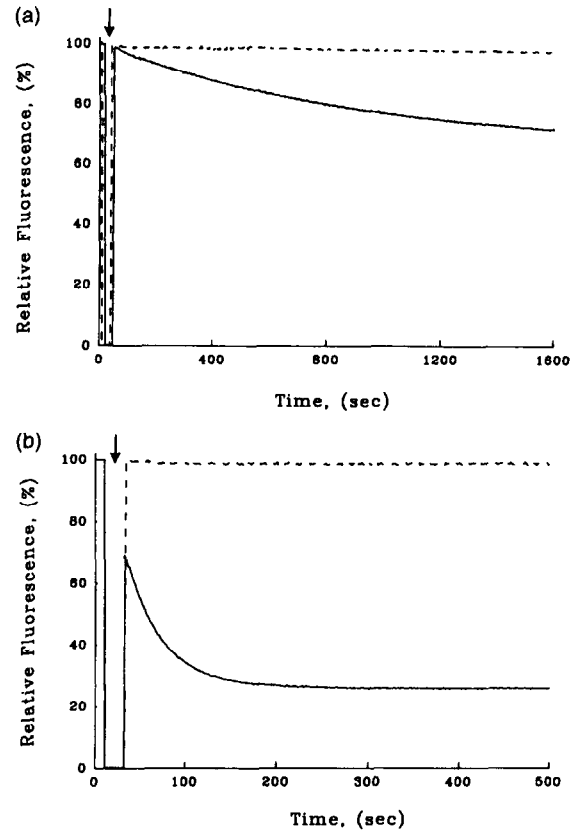

Fig. 1. Stability of the (- - -) S1 · εADP · AlF_4^- and (—) S1 · εADP · BeF_x complexes in the presence of (a) $MgCl_2$ or (b) $CaCl_2$ as determined by ADP chase. S1 (5.0 μM for the Mg complexes and 25 μM for the Ca complexes) in 40 mM KCl and 25 mM PIPES, pH 7.0 was incubated with $MgCl_2$ or $CaCl_2$ (2 mM), εADP (20 μM), $AlCl_3$ (500 μM) and NaF (10 mM) or $BeCl_2$ (200 μM) and NaF (5 mM) for 30 min. At the time indicated by the arrow, ADP (2 mM) was added. The fluorescence intensities were measured in the presence of acrylamide (100 mM). The excitation and emission wavelengths were 315 nm and 415 nm, respectively. The calculated dissociation rates of εADP from the complexes were: $1.14 (\pm 0.02) \times 10^{-5}$ s^{-1}, $1.94 (\pm 0.01) \times 10^{-4}$ s^{-1}, $1.15 (\pm 0.01) \times 10^{-5}$ s^{-1}, and $2.11 (\pm 0.03) \times 10^{-2}$ s^{-1} for S1 · Mg εADP · AlF_4^-, S1 · Mg εADP · BeF_x, S1 · Ca εADP · AlF_4^-, and S1 · Ca εADP · BeF_x, respectively.

The fast release of BeF_x from S1 · Ca εADP · BeF_x is inconsistent with earlier studies reporting the inhibitory effect of BeF_x on both Ca^{2+}– and K^+(EDTA)–ATPase of S1 [20,21]. To reconcile the ADP chase result with Ca^{2+}–ATPase measurements, the Ca^{2+}–ATPase activities of the S1 · Ca εADP ·

Table 1
Relative Ca^{2+}-ATPase activities of S1·ADP complexes with phosphate analogs BeF_x and AlF_4^-

Ca^{2+} complexes	Relative Ca^{2+}-ATPase (%)
S1·εADP	100
S1·εADP·BeF_x	95±5
S1·εADP·AlF_4^-	35±10

S1 (25 μM) in 40 mM KCl and 25 mM PIPES, pH 7.0 was incubated with $CaCl_2$ (2 mM), εADP (20 μM), $AlCl_3$ (500 μM) and NaF (10 mM) for 30 min. Prior to ATPase measurements, the S1 solution was diluted to a final concentration of 0.125 μM. The ATPase assay was initiated by the addition of ATP (2 mM) and carried out for 10 min at 37°C. ATPase activities were determined according to Kielley and Bradley [10].

BeF_x and S1 · CaεADP · AlF_4^- complexes were monitored under conditions similar to the chase experiments. It is pertinent to note that no Mg^{2+} was present in the incubation mixture or in the ATPase assays. Table 1 shows the relative Ca^{2+}-ATPase activities of the S1 · CaεADP · analog complexes. Consistent with the ADP chase results, the Ca^{2+}-ATPase activity of the S1 · CaεADP · AlF_4^- complex was strongly inhibited while BeF_x had only a marginal effect on the Ca^{2+}-ATPase activity of S1. The discrepancy between our results and the earlier reports on the inhibitory effect of BeF_x on the Ca^{2+}-ATPase activity can be attributed to the fact that in those studies the S1 · ADP · BeF_x was incubated with Mg^{2+}- prior to Ca^{2+}-ATPase measurements. Thus, S1 · MgεADP · BeF_x and not S1 · CaεADP · BeF_x was the stable complex used in the previous ATPase assays.

In contrast to S1 · CaεADP · BeF_x, which dissociated at a much faster rate than its Mg counterpart, the S1 · CaεADP · AlF_4^- complex was as stable as the S1 · MgεADP · AlF_4^- complex (Fig. 1a and b): k_{off} in both cases was 1.15 (±0.01) × 10^{-5} s^{-1}. The high stability of the S1 · CaεADP · AlF_4^- complex enabled the testing of the formation of the $S1^{**}$ · ADP · P_i state in the presence of Ca^{2+}. One way to examine this possibility is to address the question: can actin accelerate the release of products from the Ca complex? Fig. 2 shows the dissociation of AlF_4^- from the S1 · CaεADP · AlF_4^- complex induced by actin. In the presence of 30 μM actin, the rate of release of AlF_4^- from S1 · CaεADP · AlF_4^- was accelerated almost 100-fold. The acceleration of product release by actin suggests that there are no major structural differences between S1 · CaεADP · AlF_4^- and S1 · MgεADP · AlF_4^-.

3.2. Accessibility of εADP at the active site of S1 · nucleotide · analog complexes to collisional quenchers

The ADP chase (Fig. 1) and the ATPase activity (Table 1) results suggest that BeF_x and perhaps the nucleotide are in a more open environment on S1 than in the presence of AlF_4^-. This idea was tested by monitoring the accessibility of the nucleotide analog εADP in various S1 · nucleotide · analog complexes to the collisional quencher acrylamide. Fig. 3 shows the Stern–Volmer plots for acrylamide titration of εADP bound to S1 in the presence of BeF_x and AlF_4^-. In the absence of S1, the titration of εADP by acrylamide produced a straight line of F_0/F versus acrylamide concentration (data not shown), reflecting the quenching of a single species [13]. The Stern–Volmer constant of εADP in the absence of S1, obtained from the slope of such line was 55 ± 6 M^{-1}. In the presence of S1, the Stern–Volmer plot displays a downward curvature characteristic of the quenching of at least two species, the free and the

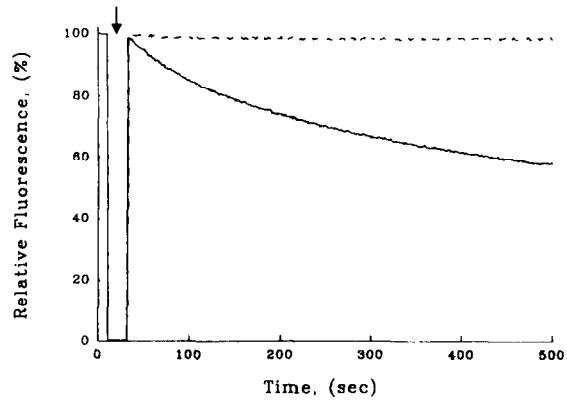

Fig. 2. Dissociation of AlF_4^- from the actoS1 · CaεADP · AlF_4^-. S1 (25 μM) in 40 mM KCl and 25 mM PIPES, pH 7.0 were incubated with $CaCl_2$ (2 mM), εADP (20 μM), $AlCl_3$ (500 μM) and NaF (10 mM) for 30 min. At the time indicated by the arrow, (---) ADP (2 mM) or (—) actin (30 μM) was added. The calculated dissociation rates of εADP by ADP and actin were: 1.14 (±0.01) × 10^{-5} s^{-1} and 1.08 (±0.01) × 10^{-3} s^{-1}, respectively.

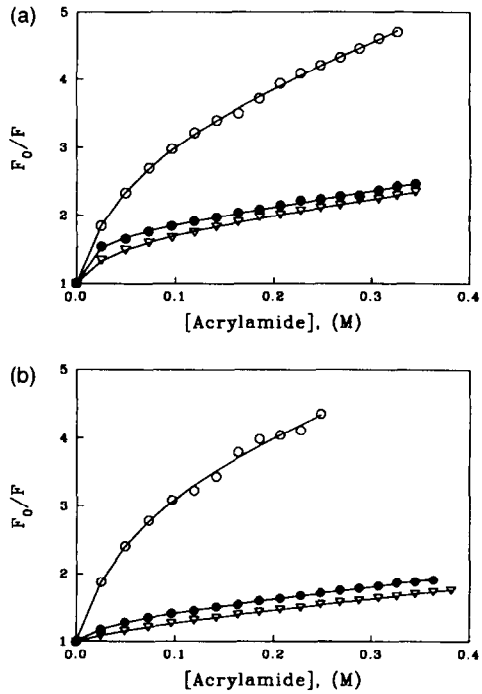

Fig. 3. Stern–Volmer plots of acrylamide titrations for (a) S1 · MgεADP and (b) S1 · CaεADP complexes with BeF_x and AlF_4^-. The accessibility of εADP to quencher was monitored by acrylamide titrations of (○) S1 · εADP, (●) S1 · εADP · BeF_x and (▽) S1 · εADP · AlF_4^-. F_o/F was determined by dividing the initial fluorescence intensity (F_o) by fluorescence intensity (F) at any given acrylamide concentration. The smooth curve drawn through the data points is the computer fit to Eq. 1 (Lakowicz, 1983):

$$F_o/F = 1/[(F_f/(1+K_f)[Q]) + (F_b/(1+K_{SV})[Q])]$$

bound εADP (Fig. 3). To obtain the quenching constant for the bound component, the titration data were fitted to Eq. 1 [13] by using the quenching constant of the free component determined in the absence of S1 ($55 \pm 6\ M^{-1}$). Both in the presence of Mg^{2+} (Fig. 3a) and Ca^{2+} (Fig. 3b), acrylamide titrations of S1 · εADP · BeF_x and S1 · εADP · AlF_4^- showed little difference in nucleotide protection between the two complexes. Indeed, the Stern–Volmer quenching constants of the bound εADP were similar for S1 · εADP · BeF_x and S1 · εADP · AlF_4^- (Table 2), suggesting that the accessibility of the bound εADP to acrylamide was the same for both complexes. Furthermore, the Stern–Volmer quenching constants of the Mg^{2+} complexes were very close to those of the Ca^{2+} complexes (Table 2), suggesting that the environment of the adenine moiety is similar for both cation-chelating complexes.

3.3. SH_1 modification by IAF

Chemical modification experiments revealed that the environment of the reactive SH_1 thiol on myosin (Cys-697) is different in the S1 · MgADP · BeF_x and S1 · MgADP · AlF_4^- complexes [6]. Thus, while the present results, as well as the recent study of Franks–Skiba et al. [4], show that ATP hydrolysis does not change the active site cleft around the adenine moiety, the SH_1–SH_2 helix on S1 appears to be more sensitive to γ-phosphate cleavage. To confirm that changes at the phosphate site induce conformational changes at the SH_1 site, S1 was labeled with the monofunctional reagent IAF. The emission spectra of IAF-labeled S1 were recorded in the presence of various nucleotides and analogs. The comparison of such emission spectra was justified by earlier studies [22,23] which showed that SH_1 modifications of S1 did not change its properties other than altering the rates of interconversion between kinetic intermediates of the ATPase reaction and the distribution of their populations. The addition of MgADP, ATP, ATPγS and ADP + BeF_x did not have any measurable effect on the emission intensity

Table 2
Stern–Volmer constants (K_{SV}) for S1 · εADP complexes in the presence of Ca^{2+} and Mg^{2+}

Cation	Protein complexes [a]	εADP bound (%) [b]	K_{SV} (M^{-1}) [c]
Ca^{2+}	S1 · εADP	68 ± 5	1.50 ± 0.06
	S1 · εADP · BeF_x	92 ± 6	1.30 ± 0.05
	S1 · εADP · AlF_4^-	95 ± 4	1.20 ± 0.06
Mg^{2+}	S1 · εADP	64 ± 5	1.55 ± 0.17
	S1 · εADP · BeF_x	74 ± 7	1.30 ± 0.06
	S1 · εADP · AlF_4^-	81 ± 6	1.26 ± 0.07

[a] The protein complexes were formed as described in Materials and Methods.
[b] The fraction of nucleotide that was bound to S1 was measured following sedimentation of a portion of the sample through a semipermeable membrane that allowed passage of the free nucleotide but not that of the protein and bound nucleotide.
[c] K_{SV} values referring to the quenching constant of the bound nucleotide in the protein complexes were obtained by fitting the data to Eq. 1 [13]. The Stern–Volmer constant for the free nucleotide (in the absence of S1) was $55 \pm 6\ M^{-1}$.

of IAF-labeled S1. However, the addition of ADP and AlF_4^- increased the emission intensity of IAF-labeled S1 at 520 nm by $25 \pm 5\%$ (Fig. 4). These results suggest conformational differences at the SH_1 site between the S1 · MgADP · BeF_x and S1 · MgADP · AlF_4^- complexes.

3.4. Probing the conformational change at the SH_2 site

To probe the conformational change at the SH_2 site induced by changes at the phosphate site, the SH_2 thiol was labeled with IANBD. The choice of this modifying reagent is based on the observation that it can specifically modify SH_2 in the presence of MgADP and actin [15,21]. Thus, no preblocking of the more reactive SH_1 site is required. The labeled S1 was separated from actin by salt increase, ATP addition and ultracentrifugation. The specificity of labeling was verified by K^+(EDTA)– and Ca^{2+}–ATPase measurements.

The conformational changes in the SH_2-labeled S1 were examined by monitoring the emission spectra of the IANBD–S1 in the presence of different nucleotides and analogs (Fig. 5). The addition of

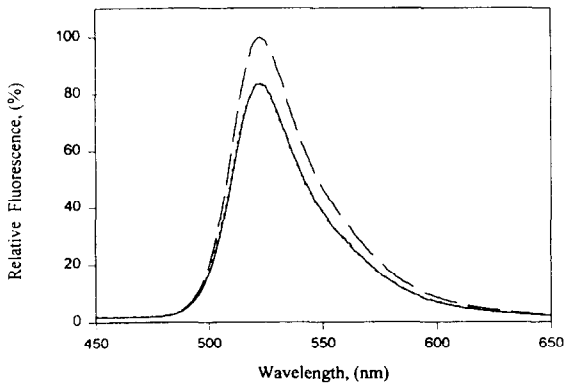

Fig. 4. Emission spectra of IAF-labeled (—) S1 · MgADP, (- - -) S1 · MgADP · AlF_4^- and (---) S1 · MgADP · BeF_x. The SH_1 modification of S1 by IAF was carried out as described in Materials and Methods. The IAF-labeled S1 was incubated with MgADP (2 mM), $AlCl_3$ (500 μM) and NaF (10 mM) or $BeCl_2$ (200 μM) and NaF (5 mM) for 30 min prior to emission scans. The excitation wavelength was set at 365 nm. The emission spectra of IAF-labeled S1 in the presence of ATP, ATPγS and in the absence of nucleotide (not shown) were similar to that of IAF-labeled S1 · MgADP and S1 · MgADP · BeF_x.

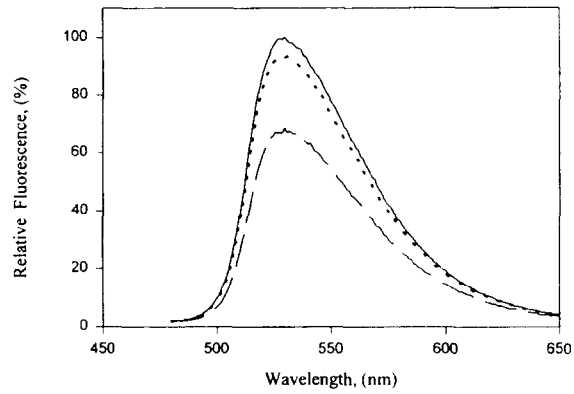

Fig. 5. Emission spectra of IANBD-labeled (—) S1 · MgADP, (- - -) S1 · MgADP · AlF_4^- and (---) S1 · MgADP · BeF_x. The SH_2 modification by IANBD was carried out as described in Materials and Methods. The IANBD-labeled S1 was incubated with MgADP (2 mM), $AlCl_3$ (500 μM) and NaF (10 mM) or $BeCl_2$ (200 μM) and NaF (5 mM) for 30 min prior to emission scans. The excitation wavelength was set at 472 nm. The emission spectra of IANBD-labeled S1 in the presence of ATP, ATPγS and in the absence of nucleotide (not shown) were similar (within experimental error) to that of IANBD-labeled S1 · MgADP.

MgADP, ATP and ATPγS did not induce any measurable change in the emission spectrum of IANBD-labeled S1. In the presence of ADP and BeF_x, the emission intensity of SH_2-labeled S1 at 525 nm decreased by $5 \pm 2\%$. Upon addition of ADP and AlF_4^-, the emission intensity of the labeled S1 decreased by over $30 \pm 5\%$. The lack of a similar perturbation of the probe in the presence of ATP can be attributed to the possibility that SH_2 modification may change the distribution of S1 · ATP, S1** · ADP · P_i and S1 · ADP in the S1 and ATP mixture. Therefore, the predominant species in the mixture may no longer be the S1** · ADP · P_i complex. The fluorescence difference in the emission spectra of SH_2-labeled S1 · MgADP · BeF_x and S1 · MgADP · AlF_4^- suggests conformational differences at the SH_2 site between these two complexes.

4. Discussion

It has been a long standing goal in muscle biochemistry to obtain a structural description of the intermediate complexes along the ATP hydrolysis pathway. The arsenal of ATP and phosphate analogs

available for such purpose has recently increased with the addition of BeF_x and AlF_4^- as stable phosphate analogs [19–21,24]. In complexes with S1 and MgADP the two analogs appear to yield conformationally different states, as suggested by photolabeling and nuclear magnetic resonance (NMR) experiments [25–27]. Chemical modification studies of the reactive SH_1 group on S1 suggested that the conformational states of S1 · ADP · BeF_x and S1 · ADP · AlF_4^- correspond to prehydrolyzed state S1 · ATP and transition state S1** · ADP · P_i, respectively [6].

The most recent crystallographic study of S1dC · MgADP · BeF_x and S1dC · MgADP · AlF_4^- indeed revealed structural differences between these complexes [5]. The former complex was similar to the structure of the unliganded, methylated S1, while the structure of S1dC · MgADP · AlF_4^- suggested domain movements and changes in the SH_1–SH_2 region. The geometry of the S1 · MgADP · BeF_x and S1 · MgADP · AlF_4^- complexes correspond to the bond lengths expected for S1 · MgATP and S1** · MgADP · P_i analog states. Strikingly, and in agreement with fluorescence quenching experiments of nucleotide analogs [4], no significant changes in the opening of the cleft were detected between the three solved structures of myosin heads S1, S1dC · MgADP · BeF_x and S1dC · MgADP · AlF_4^-. Yet, space filling models of the last two structures strongly suggest that BeF_x, and by analogy ATP, are accessible to solvent while the AlF_4^- complex, and thus the corresponding transition state in ATP hydrolysis, appear to be buried [5].

Solution studies of S1 · εADP · BeF_x and S1 · εADP · AlF_4^- complexes carried out in this work did not reveal any significant differences in solvent accessibility of the adenine moiety of εADP in these structures. Stern–Volmer coefficients for εADP quenching by acrylamide were virtually identical in both Mg^{2+} and Ca^{2+} complexes of S1 · εADP · BeF_x and S1 · εADP · AlF_4^-. This is significant since the off rates of BeF_x and AlF_4^- differed widely, over three orders of magnitude, between the most stable (S1 · MgεADP · AlF_4^-) and least stable (S1 · CaεADP · BeF_x) complexes of S1. Thus, while the environment of phosphate moiety or the bonding of the phosphate analog to S1 is clearly different in the S1 · εADP · BeF_x and S1 · εADP · AlF_4^- complexes, the adenine site appears invariant. This result is consistent with the recent hypothesis on the "back door" exit channel for the hydrolyzed phosphate from S1 [28]. If indeed P_i "exits" S1 via a separate channel, conformational changes in the adenine and phosphate sites need not be tightly coupled.

The use of Ca–nucleotide complexes in our experiments, to extend the stability range of the analogs of the S1** · ADP · P_i and S1 · ATP states merits a comment. The turnover rate of Ca–ATPase activity of myosin is about two orders of magnitude faster than that of MgATP hydrolysis. This means that a much smaller fraction of kinetic intermediates will be accumulated in the S1** · ADP · P_i state in the presence of Ca^{2+} than in the presence of Mg^{2+}. This fact could account for the inability of Ca–ATP to support the contractile process. However, it is also possible that the transition state intermediate in the Ca–ATPase pathway has a different conformation than S1** · MgADP · P_i and thus, actin cannot accelerate P_i release and trigger force-transducing changes in S1. The observation that actin accelerated the off rate of AlF_4^- from the stable S1 · CaεADP · AlF_4^- complex by two orders of magnitude shows that kinetic and not structural reasons are responsible for the lack of Ca–ATPase activation by actin. This conclusion validated the analysis of quenching titration of S1 · CaεADP · BeF_x and S1 · CaεADP · AlF_4^- complexes in the same terms as for the Mg^{2+} counterparts, i.e. states analogous with S1 · ATP and S1** · ADP · P_i.

According to the present understanding of the S1 · ADP · BeF_x and S1 · ADP · AlF_4^- complexes as the analogs of S1 · ATP and S1** · ADP · P_i states, the different off rates of BeF_x and AlF_4^- from these complexes reflect ATP hydrolysis linked changes in the phosphate site of the active cleft. Although, as shown in this and previous work [4], such changes do not alter the adenine site, they significantly change the reactivity of the SH_1 group on S1 [6]. We show in this work, by monitoring emission spectra of fluorescent probes attached to SH_1 and SH_2 groups, that the environment of both residues, and perhaps that of the entire 697–707 helix is changed upon P_i cleavage. Structural differences in this region have indeed been observed between the S1dC · MgADP · BeF_x and S1dC · MgADP · AlF_4^- crystals [5]. These results substantiate the hypothesis that changes in the SH_1–SH_2 region of S1 are important for signal

transduction between the nucleotide and actin sites [29,30] and the motor function of myosin.

An obvious question, related to the proposed model for the mechanism by which S1 translocates actin filaments, is whether the changes in the phosphate and SH_1–SH_2 sites on myosin produce the bending of S1 at the yet unidentified hinge residue [5]. Hydrodynamic bead modeling of the S1 molecule using the program HYDRO [31] to estimate changes in the translational and rotational frictional coefficients of S1 for various degrees of bending of the regulatory domain relative to the catalytic domain has led to the conclusion that relatively large changes ($< 45°$) could easily escape detection by methods that effectively measure the translational frictional coefficient. Modeling of S1 with a straight and bent tail (45°) showed that almost no change in sedimentation coefficient ($< 1\%$) would be observed. As predicted by such modeling, difference sedimentation measurements on S1 complexes with phosphate analogs showed no differences larger than 1%. On the other hand, methods that measure rotational relaxation times, like fluorescence anisotropy decay and transient electric birefringence are expected to be much more sensitive to S1 bending. Indeed, electric birefringence [32,33] and low-angle X-ray scattering [34] measurements detected small changes in S1 with ATP hydrolysis. This change led Highsmith and Eden [33] to propose a bending of S1, independent of and prior to crystallographic work, as a main feature of the myosin motor action.

Acknowledgements

This work was supported by USPHS Grant AR 22031 (E.R.), American Heart Association Research Fellowship 1045 FI 1 (B.C.P.) and NSF Grant MCB 9206739 (E.R.).

References

[1] W.F. Harrington, E. Reisler and M. Burke, J. Supramol. Struct., 3 (1975) 112.
[2] I. Rayment and H.M. Holden, Trends Biochem. Sci., 19 (1994) 129.
[3] T. Hiratsuka, J. Biol. Chem., 269 (1994) 27521.
[4] K. Franks-Skiba, T. Hwang and R. Cooke, Biochemistry, 33 (1994) 12720.
[5] A.J. Fisher, C.A. Smith, J. Thoden, R. Smith, K. Sutoh, H.M. Holden and I. Rayment, Biophys. J., 68 (1995) 19S.
[6] B.C. Phan and E. Reisler, Biochem. J., 66 (1994) A78.
[7] J.E. Godfrey and W.F. Harrington, Biochemistry, 9 (1970) 886.
[8] A.S. Weeds and B. Pope, J. Mol. Biol., 111 (1977) 129.
[9] J.A. Spudich and S. Watt, J. Biol. Chem., 246 (1971) 4866.
[10] W.W. Kielley and L.B. Bradley, J. Biol. Chem., 208 (1956) 653.
[11] T. Ando, A.J. Duke, Y. Tonomura and A.F. Morales, Biochem. Biophys. Res. Commun., 109 (1982) 1.
[12] S.S. Lehrer and P.C. Leavis, Meth. Enzymol., 49 (1978) 222.
[13] J.R. Lakowicz, Principles of Fluorescence Spectroscopy, Plenum Press, New York, 1983.
[14] E. Reisler, Meth. Enzymol., 85 (1982) 84.
[15] D.D. Root and E. Reisler, Biophys. J., 63 (1992) 730.
[16] C.R. Bagshaw and D.R. Trentham, Biochem. J., 133 (1973) 323.
[17] R.W. Lymn and E.W. Taylor, Biochemistry, 17 (1970) 2975.
[18] E.W. Taylor, R.W. Lymn and G. Moll, Biochemistry, 17 (1970) 2984.
[19] B.C. Phan, L.D. Faller and E. Reisler, Biochemistry, 32 (1993) 7712.
[20] B.C. Phan and E. Reisler, Biochemistry, 31 (1992) 4787.
[21] K. Ajtai and T. Burghart, Biochemistry, 28 (1989) 2204; M.M. Werber, Y.M. Peyser and A. Muhlrad, Biochemistry, 31 (1992) 7190.
[22] J.A. Sleep, K.M. Trybus, K.A. Johnson and E.W. Taylor, J. Muscle Res. Cell Motil., 2 (1981) 373.
[23] E.M. Ostap, H.D. White and D.D. Thomas, Biochemistry, 32 (1993) 6712.
[24] A.A. Bobkov, N.V. Khvorov, N.L. Golitsina and D.I. Levitsky, FEBS Lett., 332 (1993) 64.
[25] S. Maruta, G.D. Henry, B.D. Sykes and M. Ikebes, J. Biol. Chem., 268 (1993) 7093.
[26] R. Takashi, M. Ikebe and S. Maruta, Biophys. J., 64 (1993) A143.
[27] S. Maruta, Biophys. J., 66 (1994) A75.
[28] R.G. Yount, D. Lawson and I. Rayment, Biophys. J., 68 (1956) 44S.
[29] J. Botts, J.F. Thomason and M.F. Morales, Proc. Natl. Acad. Sci. USA, 86 (1989) 2204.
[30] T. Hiratsuka, J. Biol. Chem., 269 (1992) 14941.
[31] J. Garcia de la Torre, S. Navaro, M.C. Lopez Cascales, F.G. Diaz and J.J. Lopez Cascales, Biophys. J., 67 (1994) 530.
[32] S. Highsmith and D. Edan, Biochemistry, 29 (1990) 4087.
[33] S. Highsmith and D. Edan, Biochemistry, 32 (1993) 2455.
[34] Y. Sugimoto, M. Tokunaga, Y. Takazewa, M. Ikebe and K. Wakabayashi, Biophys. J., 68 (1995) 29S.